Nitrogen ion irradiation of Au(110): Photoemission spectroscopy and possible crystal structures of gold nitride

S. Krishnamurthy,[1] M. Montalti,[1] M. G. Wardle,[2] M. J. Shaw,[2] P. R. Briddon,[2] K. Svensson,[3] M. R. C. Hunt,[4] and L. Šiller[1,*]

[1]*School of Chemical Engineering and Advanced Materials, University of Newcastle upon Tyne, Newcastle upon Tyne NE1 7RU, United Kingdom*

[2]*School of Natural Sciences, University of Newcastle upon Tyne, Newcastle upon Tyne NE1 7RU, United Kingdom*

[3]*Applied Physics Department, Chalmers University of Technology, Göteborg SE-41296, Sweden*

[4]*Department of Physics, University of Durham, Durham DH1 3LE, United Kingdom*

(Received 12 November 2003; revised manuscript received 23 March 2004; published 21 July 2004)

Photoemission spectroscopy demonstrates the formation of a surface gold nitride upon irradiation of a Au(110) surface with 500 eV nitrogen ions at room temperature. After irradiation two N1*s* peaks are observed at binding energies of 396.7 ± 0.2 eV and 397.7 ± 0.2 eV along with a broadening of the Au4$d_{5/2}$ line. Changes in valence-band spectra are also observed, including an additional density of states at 1.6 eV binding energy and new states at ~ 3.1 eV. Annealing experiments indicate that the two N1*s* lines are associated with nitrogen compounds of differing thermal stability, possibly due to the formation of more than one nitride phase. To further investigate the properties of gold nitride we have undertaken *ab initio* pseudopotential calculations on the most likely nitride stoichiometry, Au_3N, and identified a novel triclinic crystal structure of a significantly lower energy than the *anti*-ReO_3 expected from a simple consideration of the periodic table, although the latter structure is also found to be stable. The triclinic structure is determined to be metallic, of importance to possible applications.

DOI: 10.1103/PhysRevB.70.045414 PACS number(s): 79.60.Dp, 81.15.Cd, 61.50.Ah

INTRODUCTION

Metal nitrides are technologically important compounds and have a wide range of applications including as electron field emitters[1,2] and catalysts for various reactions.[3,4] Over the years there has been a considerable effort directed towards the formation and study of noble metal nitrides such as copper, silver, and gold nitrides. However, until a short time ago, there had been clear evidence only for the formation of copper and silver nitrides.[5–11] Although attempts to form gold nitrides have been recorded for the past 20 years, this compound has been observed only recently by Šiller *et al.*[12] In that work, irradiation of a gold surface with low-energy (500 eV) nitrogen ions was used to produce a surface nitride layer which was then investigated with high-resolution x-ray photoelectron spectroscopy. Two N1*s* core lines were observed after irradiation. Using angle-resolved measurements these two lines were interpreted in terms of nitrogen chemically bound to gold and molecular nitrogen trapped beneath the gold surface in bubbles. It has been suggested[12] that the main reasons why previous research had not been able to produce/detect gold nitrides are that the incident ion energies employed were too high and/or that the sensitivity of the analytical techniques used in those studies was not sufficient.

In the work reported here we employ synchrotron radiation excited photoemission spectroscopy (PES) to study the core lines of both Au and N after ion irradiation and to examine changes in valence-band spectra induced by nitride formation. The high signal and resolution which are offered by synchrotron based PES measurements enable us to identify changes in the Au4*d* line associated with irradiation and to resolve two components associated with chemically bound nitrogen, which have not been previously detected. *Ab initio* density-functional theory (DFT) calculations are used to determine the structure, stability, and electronic properties of gold nitride structures of the most likely stoichiometry, Au_3N. We find that the most stable structure is a novel triclinic crystal structure of a significantly lower energy than the *anti*-ReO_3 expected from a simple consideration of the periodic table. This structure is determined to be metallic, of importance to possible applications.

EXPERIMENTAL

Experiments were performed using the vacuum ultraviolet beamline at the ELETTRA synchrotron radiation facility in Trieste, Italy. The end station consists of a two chamber ultrahigh vacuum system with a base pressure better than 5×10^{-10} mbar. The preparation chamber contains an annealing stage, mass spectrometer, low-energy electron-diffraction (LEED) optics, and a differentially pumped ion gun. An Omicron EA125 hemispherical electron energy analyzer mounted in the analysis chamber was used to record the photoemission spectra. Nitride films were formed on the (110) surface of a gold single crystal which was cleaned *in situ* by sputtering with Ar ions of kinetic energy 500 eV for 35 min. The sample was then annealed at 500 °C for 30 min to restore surface crystallinity. The cleanliness and crystallinity of the sample were then examined with PES and LEED, respectively.

In order to form a surface nitride layer the Au(110) surface was exposed to nitrogen ion irradiation using an ion kinetic energy of 500 eV. The ion gun was fed with 99.999%

pure N_2 gas and adjusted to ensure that the entire surface of Au crystal was evenly irradiated. During the implantation the chamber pressure rose to 1×10^{-5} mbar. A quadrupole mass spectrometer was used to monitor the composition of the chamber gas during implantation—no significant rise of the signals due to water or carbon monoxide were observed. Mass spectroscopy indicated that the dominant ion species was N^+, however, there was no control or selection of the ion species impinging upon the gold surface during irradiation, and in consequence N_2^+ ions may also be present.

Irradiation was performed at normal incidence with measured ion currents of 3.5–4 μA, and the sample was held at room temperature. Core-level photoemission studies were performed using a photon energy of 500 eV, while valence-band measurements employed a photon energy of 40 eV. The total resolution for core level is 0.15 eV and for valence band is 50 meV. Binding energies in core-level spectra were calibrated by taking the binding energy of the main Au4$d_{5/2}$ line as 334.8 eV (Ref. 13) while binding energies valence-band spectra were referred to the Fermi level of the sample. Core-level spectra were obtained at grazing emission (75° off normal) unless otherwise stated, while valence-band spectra were acquired in normal-emission geometry.

RESULTS AND DISCUSSION

In Fig. 1(a) a N1*s* core-level photoemission spectrum obtained from an Au(110) surface irradiated with 500 eV nitrogen ions to a dose of 4990 μC is presented. Two peaks, at binding energies 396.7 ± 0.2 eV and 397.7 ± 0.2 eV can be observed, with the binding energy values obtained by fitting the peaks with Gaussian-Lorentzian line shapes and a Shirley background. The peak at 396.7 ± 0.2 eV has a binding energy very close to that observed for chemisorbed nitrogen on Cu(110), which lies in the range 396.5–396.8 eV, depending upon coverage[14] and has been previously assigned to the presence of nitrogen chemically bound to Au.[12] The second component was not previously resolved due to the lower resolution and signal-to-noise ratio available in the original measurements.[12] Both peaks have approximately the same area, but their different widths are reflected in differing peak heights. Spectra from the same surface obtained in normal-emission geometry show the same peak position and line shape, but a larger overall intensity. However, due to the roughness inherent in the irradiated surface it is not possible to reach a conclusion regarding the uniformity of the near-surface region of the sample. Based upon the broadening of the Au4$d_{5/2}$ line, discussed below, we estimate that the upper limit for Au in the form of AuN_x within the probe depth of our experiment is ~18% (given surface roughness, we expect the probe depth to be between ~1 nm at grazing emission and ~3 nm at normal emission for a smooth surface). Calculations using SRIM-2000 (Ref. 15) indicate that N ions with 500 eV kinetic energy penetrate to an average depth of ~2 nm suggesting that nitride formation in the near-surface region is incomplete in the irradiation dose range studied and that the surface region most likely consists of both unreacted gold and gold nitride (for complete nitride formation we would expect, from the differing depths associated with ion penetration and electron inelastic mean free path, that ~60–100% of the gold detected in core-level spectra should be in the form of a nitride).

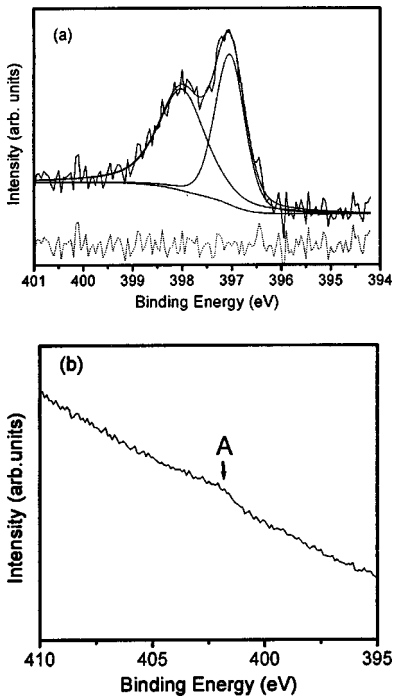

FIG. 1. (a) N1*s* core-level spectrum obtained from an Au(110) surface exposed to a nitrogen ion dose of 4990 μC at 500 eV, obtained in grazing emission, after subtraction of a sloping linear background. The experimental curve is fitted to two Gaussian-Lorentzian singlets and a Shirley background. The dotted curve at the bottom of the Figure is a plot of the fit residuals. (b) N1*s* core-level spectrum obtained from an Au(110) surface exposed to a nitrogen ion dose of 900 μC at 2 keV, obtained in grazing emission.

A N1*s* core-level spectrum obtained from an Au(110) surface exposed to a nitrogen ion dose of 900 μC at 2 keV and 300 K is shown in Fig. 1(b). The N1*s* line assigned to gold nitride is absent. A weak feature, labeled *A*, is observed at a binding energy of 402.2 ± 0.1 eV. This peak has also been detected in previous experiments,[12] and was assigned to the presence of molecular nitrogen trapped beneath the surface of the gold, in the form of bubbles. The absence of the core line associated with the formation of gold nitride in this spectrum can be attributed to the higher incident energy employed during irradiation of this sample. Upon irradiation, nitride formation and implantation compete with sputtering of surface material, and at sufficiently high incident ion energy the latter process can dominate. The absence of any core lines associated with chemisorbed nitrogen species at higher incident ion energies indicates that these species are unlikely to arise from contamination during the irradiation process.

Changes in the Au4$d_{5/2}$ line shape were also observed after nitrogen ion irradiation, and Fig. 2 shows the results of irradiation to an ion dose of 4990 μC at 500 eV. A clear broadening of the Au4$d_{5/2}$ peak towards higher binding energies with nitrogen ion bombardment is seen. Examination of Au4$d_{5/2}$ spectra obtained from clean samples irradiated

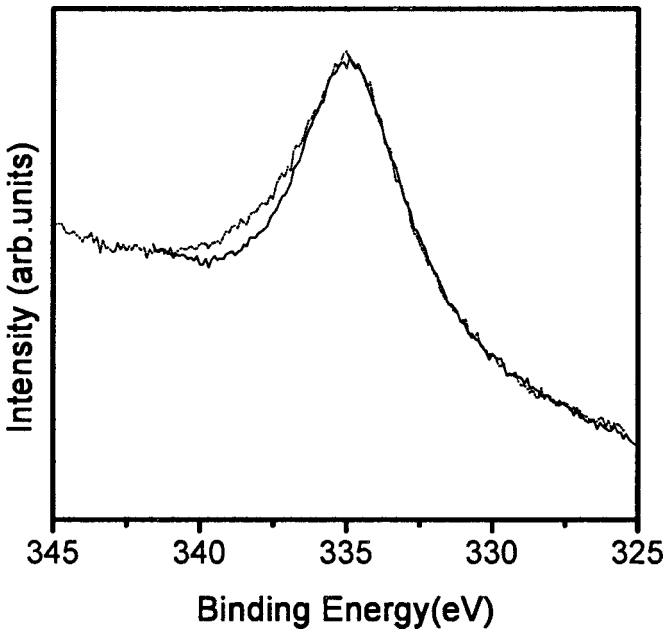

FIG. 2. Au4*d* core-level spectra before (solid line) and after (dotted line) a nitrogen ion dose of 4990 μC at 500 eV taken at grazing emission.

with Ar ions show a similar broadening prior to annealing. Although the high binding energy broadening of the Au4$d_{5/2}$ line after nitrogen ion irradiation appears larger than that for Ar irradiation, it is impossible to accurately disentangle the effects of surface roughness from those which may be associated with a new component arising from reaction with nitrogen. Since a substantial proportion of the Au4*d* signal arises from gold which is not bound to nitrogen we cannot, at present, experimentally determine the stoichiometry of the gold nitride phase(s). However, as mentioned above, the broadening of the Au4$d_{5/2}$ line does enable us to place an *upper limit* of ~18% on the fraction of gold chemically bound to nitrogen over the probe depth of the photoemission experiment. In Fig. 3, N1*s* spectra for nitrogen ion doses of 4990 μC and 500 μC at 500 eV (triangles and circles, respectively) are presented. As expected a rise in both components as a function of increasing ion dose is observed. From the data it appears that both components grow equally rapidly as a function of ion dose, although further measurements are required at low doses to verify that the ratio of the N1*s* peaks remains constant over the nitride formation process.

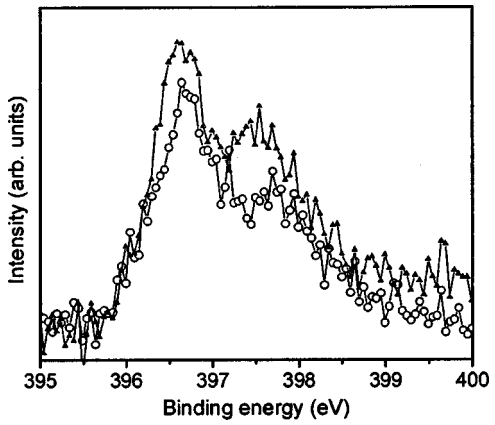

FIG. 3. N1*s* core-level spectra obtained from an Au(110) surface exposed to nitrogen ion doses of 4990 μC and 500 μC at 500 eV, open circles and triangles, respectively, obtained in grazing emission.

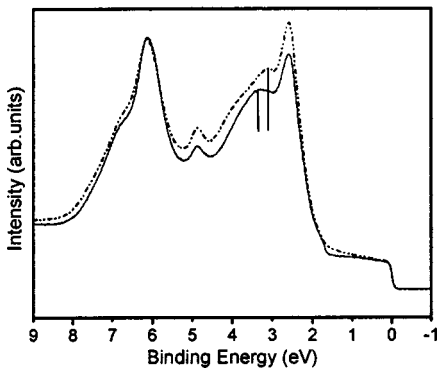

FIG. 4. Comparison of valence-band spectra before (solid line) and after (dotted line) a nitrogen ion dose of 4990 μC at 500 eV. Spectra were obtained in normal emission with photon energy $h\nu$ = 40 eV. The vertical bars show changes in the peak structure in the *d*-band region.

In Fig. 4 valence-band spectra before (solid line) and after (dotted line) a nitrogen ion dose of 4990 μC at 500 eV are presented. A tail in the valence-band intensity close to the Fermi level is observed in the energy range 0.1–1.8 eV in addition to a new peak at 3.1 eV (denoted by an arrow). It is known that a surface state of *d*-type character is located near the $\mathbf{\Gamma}$ point along $\mathbf{\Gamma}$-$\mathbf{X}$[16,17] on Au(110) surfaces. Upon sputtering and ion implantation into the gold crystal, the surface becomes rough and these surface states will be strongly modified, which may explain the appearance of this broad "tail" in the spectra. The new state at 3.1 eV might be due to nitrogen-gold bonding (see discussion of theoretical data below).

Annealing experiments were undertaken on a sample irradiated with an ion dose of 770 μC to explore the stability of the surface gold nitride, as shown in Fig. 5 (obtained in normal-emission geometry). Before considering the effects

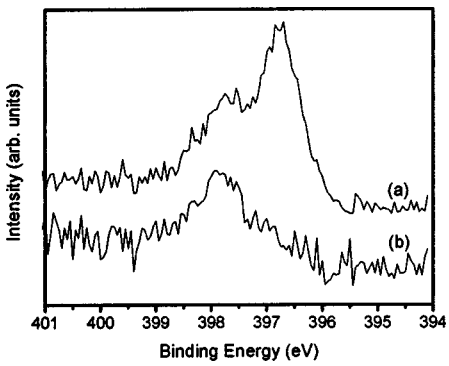

FIG. 5. (a) N1*s* spectrum from a gold nitride film formed by a nitrogen ion dose of 770 μC at 500 eV. (b) N1*s* spectrum obtained after annealing the sample at ~200 °C. Both spectra were obtained in normal-emission geometry.

of annealing itself, it is worth noting that the lower ion dose produces N1*s* lines with a similar ratio, line shape, and area to that observed for the 4990 μC ion dose. This suggests that the surface nitride is formed in an equilibrium in which a steady rate of formation is balanced by erosion of the surface through ion sputtering. The observation that higher irradiation energies do not lead to nitride formation, as discussed above, reinforces the assertion that higher rates of sputtering at increased ion energies prevent the formation of observable quantities of gold nitride. Upon annealing to $\sim$200 °C the lower binding energy N1*s* component is strongly reduced in intensity, indicating that the nitrogen species associated with the two N1*s* lines have significantly different stability. Since we took the spectra shown in Fig. 5 in normal-emission geometry which is bulk sensitive (electron escape depth $\sim$3 nm), we suggest that most probably the species associated with the lower binding energy N1*s* component desorbs rather than diffuses into the bulk of the sample. We can, therefore, draw the conclusion that the N1*s* lines are most probably associated with nitrogen atoms in different bonding configurations (and possibly phases) within the surface layer and that the nitride phase associated with lower binding energy has a limited thermal stability.

To further investigate the nature of the nitride phase(s) formed during ion implantation we have undertaken *ab initio* studies. The stability of Cu_3N (Ref. 18) and Ag_3N (Ref. 19) suggests that a Au_3N stoichiometry is a good starting point for further investigation. Using DFT with first-principles pseudopotentials it is possible to directly compare the total energy for different Au_3N crystal structures, including complex crystal structures with bases consisting of many Au_3N units, and to identify the optimum lattice parameters for these structures. In this paper we present results for a wide range of possible Au_3N structures obtained using the AIMPRO code,[20] in which a Gaussian orbital basis set is used with the separable dual-space pseudopotentials of Hutter *et al.*[21] Although we are able to compare a large number of different structures, and to identify those with lowest energy, it is of course not possible to be sure that the global minimum has been located (we can sample only a finite subset of the infinite parameter space available). What we can do, however, is examine a wide range of structures which might be expected to be of low energy (for example, those which other A_3B compounds assume), to identify which of those are the most likely candidates for the true crystal structure, and to eliminate those structures which are not energetically favorable.

The starting point for our study of possible Au_3N structures is the so-called *anti*-ReO_3 structure as established for Cu_3N.[18,22,23] From their positions in the periodic table one might expect gold nitride to be similar to copper nitride, and to take on this crystal structure. In addition, a wide range of structures corresponding to other known inorganic crystals were studied,[24] including the cubic structures of Fe_3Al, GeV_3, and skutterudite (with a $Au_{24}N_8$ basis), and the hexagonal close packed structure of RhF_3. For each structure the total energy was minimized with respect to lattice parameters and atom positions within the unit cell. The stability of structures was also tested by perturbing the atom positions and seeing whether the structure would recover. The volume of the parameter space sampled was further increased by performing total-energy minimization in which the lattice vectors were allowed to change freely, optimizing lattice symmetry and dimensions simultaneously.

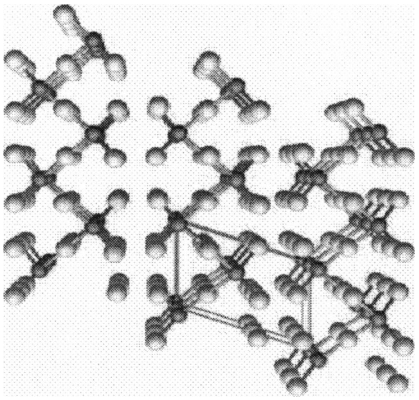

FIG. 6. The triclinic structure for Au_3N, which we find at the lowest energy of those considered. The primitive unit cell is indicated.

The *anti*-ReO_3 structure, a simple cubic structure with the lattice parameter 8.010 a.u., was indeed found to be a stable form for Au_3N. However, this was not found to be the lowest-energy structure for Au_3N in the parameter space sampled. A crystal structure was obtained following the relaxation of the atomic positions within a perturbed hexagonal close-packed unit cell. A further energy reduction was obtained upon combined optimization of the lattice vectors and atomic positions, in which the remaining hexagonal lattice symmetry was broken. The final lowest-energy structure, a triclinic lattice with a two unit basis, is shown in Fig. 6 and its primitive unit cell basis vectors are listed in Table I. This structure has a total energy of 1.0 eV per Au_3N unit below that of the *anti*-ReO_3 structure.

Although the triclinic and *anti*-ReO_3 structures of Au_3N are found to be stable with respect to perturbation of the geometric position of the atoms within the respective unit cells, it is found that both structures are about 3.25 eV higher in energy than metallic gold and molecular nitrogen per Au_3N unit cell. The instability of the gold nitride structures with respect to gold metal and N_2 indicates why a stimulated reaction is necessary to form the (metastable) phase(s) observed in the photoemission experiments. The observation, in experiment, of two distinct N1*s* lines associated with nitrogen species with differing thermal stabilities makes it tempting to assign them to different structural phases of AuN_x, given the stability of both the triclinic and *anti*-ReO_3 phases of Au_3N. However, there is also the possibility that the less

TABLE I. The primitive lattice vectors of the optimized unit cell for Au_3N. The vectors are given in atomic units as components along Cartesian axes **i**, **j**, and **k**.

Lattice vectors	**i**(a.u.)	**j**(a.u.)	**k**(a.u.)
a	8.5770580	0.0000000	0.0000000
b	4.2457181	12.093280	0.0000000
c	−0.1697887	−0.2544498	8.3046111

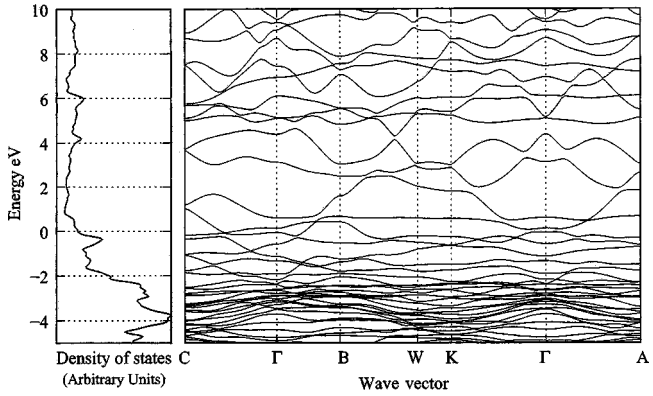

FIG. 7. The density of states and electronic band structure of the lowest-energy Au_3N structure are shown, with energy in electron volt relative to the Fermi level. The band structure is plotted along some of the symmetry lines in the Brillouin zone of the monoclinic lattice: *A* is the point $\mathbf{a}/2$, *B* is $\mathbf{b}/2$, and *C* is $\mathbf{c}/2$, where **a**, **b**, and **c** are the lattice vectors listed in Table I. *K* is the point $(\mathbf{b}+\mathbf{c})/2$ and *W* is the midpoint of the edge of the Brillouin zone at the intersections of the faces containing *B* and *K*.

stable N atoms are chemisorbed species located at the gold surface, while the more strongly bound species correspond to subsurface bulklike gold nitride.

One of the key physical properties with regard to the possible applications of gold nitride is its conductivity. The electronic band structure for the optimum structure is shown in Fig. 7 together with the associated density of states. Our model therefore predicts that the Au_3N crystal structure obtained will be metallic, in contrast to the *anti*-ReO_3 form of Au_3N which we predict to be an indirect band-gap semiconductor. It is of note that an increased density of states due to gold nitride formation with respect to pristine gold is predicted in the 3–4 eV energy region (see Fig. 7) which might correspond to the new state at observed ~3.1 eV in valence-band photoemission (Fig. 4).

CONCLUSIONS

In conclusion, photoemission investigations of Au(110) surfaces irradiated with nitrogen ions show that at sufficiently low (500 eV) incident ion energy two chemically bound nitrogen species with N1*s* lines at 396.7 ± 0.2 eV and 397.7 ± 0.2 eV binding energy can be observed. Experiments undertaken at incident ion energies of 2 keV show no chemically bound nitrogen species indicating that an increased rate of surface sputtering prevents the formation of a detectable quantity of nitride. Theoretical investigations show that for the composition of Au_3N the most energetically favorable structure is *not* the *anti*-ReO_3 structure of Cu_3N, as might be expected from a simple consideration of the periodic table, but a triclinic crystal structure of significantly lower energy. However, both structures are stable with respect to perturbation. The (meta) stability of more than one crystal structure for the Au_3N composition suggests that the different thermal stability of the two nitrogen species observed in photoemission spectra may arise from the formation of more than one gold nitride phase.

ACKNOWLEDGMENT

L.Š., M.G.W., M.J.S., and P.R.B. are grateful to EPSRC for financial support.

*Corresponding author: Electronic address: Lidija.Siller@ncl.ac.uk

[1] Y. Saito, S. Kawata, H. Nakane, and H. Adachi, Appl. Surf. Sci. **146**, 177 (1999).
[2] Y. Goth, M. Nago, T. Ura, H. Suji, and J. Ishikawa, Nucl. Instrum. Methods Phys. Res. B **148**, 925 (1999).
[3] H. Abe, T. K. Cheung, and A. T. Bell, Catal. Lett. **21**, 11 (1993).
[4] Y. C. Ma, F. Shi, and Y. Q. Deng, Prog. Chem. Toxicol. **15**, 385 (2003).
[5] L. Maya, J. Vac. Sci. Technol. A **11**, 603 (1993).
[6] G. M. Lancaster and J. W. Rabalais, J. Phys. Chem. **83**, 209 (1979).
[7] X. Zhou, H. D. Li, and B. X. Liu, J. Phys. C **21**, L-683 (1988).
[8] X. Zhou, H. D . Li, and B. X. Liu, Nucl. Instrum. Methods Phys. Res. B **39**, 583 (1989).
[9] A. Badorff and D. M. Zehner, Surf. Sci. **238**, 255 (1990).
[10] H. K. Sanghera and J. L. Sullivan, Surf. Interface Anal. **27**, 678 (1999).
[11] G. G. Tibbets, J. M. Burkstrand, and J. C. Tracey, Phys. Rev. B **15**, 3652 (1977).
[12] L. Šiller, M. R. C. Hunt, J. W. Brown, J-M. Coquel, and P. Rudolf, Surf. Sci. **513**, 78 (2002).
[13] J. C. Fuggle and N. Martensson, J. Electron Spectrosc. Relat. Phenom. **21**, 275 (1980).
[14] F. M. Leibsle, C. F. J. Flipse, and A. W. Robinson, Phys. Rev. B **47**, 15 865 (1993).
[15] J. F. Ziegler, J. P. Biersack, and U. Littmark, *The Stopping and Range of Ions in Solids* (Pergamon Press, New York, 1999).
[16] K. Stahrenberg, Th. Herrmann, N. Esser, W. Richter, S. V. Hoffmann, and Ph. Hofmann, Phys. Rev. B **65**, 035407 (2001).
[17] C. H. Xu, K. M. Ho, and K. P. Bohnen, Phys. Rev. B **39**, 5599 (1989).
[18] U. Hahn and W. Weber, Phys. Rev. B **53**, 12 684 (1996).
[19] E. S. Shanley and J. L. Ennis, Ind. Eng. Chem. Res. **30**, 2503 (1991).
[20] P. R. Briddon and R. Jones, Phys. Status Solidi B **217**, 131 (2000).
[21] C. Hartwigsen, S. Goedecker, and J. Hutter, Phys. Rev. B **58**, 3641 (1998).
[22] K. J. Kim, J. H. Kim, and J. H. Kang, J. Cryst. Growth **222**, 767 (2001).
[23] D. M. Borsa, S. Grachev, C. Presura, and D. O. Boerma, Appl. Phys. Lett. **80**, 1823 (2002).
[24] A. F. Wells, *Structural Inorganic Chemistry* (Oxford University Press, New York, 1990).